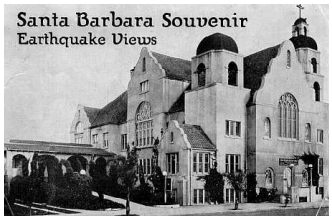

4th IASPEI / IAEE International Symposium:

Effects of Surface Geology on Seismic Motion

August 23–26, 2011 · University of California Santa Barbara

COMPUTATION OF EARTHQUAKE RESPONSES OF AN ECCENTRIC STRUCTURE USING GREEN'S FUNCTIONS RETRIEVED FROM MICROTREMORS.

Kenichi NAKANO
Kyoto University
Gokasho, Uji, Kyoto 611-0011
Japan

Masahiko MIYOSHI
Osaka Institute of Technology
Omiya, Asahi, Osaka, Osaka 535-8585
Japan

Masanori HORIKE
Osaka Institute of Technology
Omiya, Asahi, Osaka, Osaka 535-8585
Japan

ABSTRACT

The objective of our study is to retrieve Green's functions from transfer functions of buildings that satisfy the causality by transforming phase spectra to satisfy the causality. It is often the case that when we perform reverse Fourier transforms directly to transfer functions retrieved from micro-tremors in order to obtain Green's functions, we encounter the situation where the Green's function does not satisfy causality. We estimated optimal solutions of Green's functions using Generic Algorithm so that transfer functions of theoretical equation of motions fit transfer functions of observed micro-tremors. In addition, we identified the stiffness of buildings by using the identified variable of the Green's functions. We checked the condition of buildings through the identified stiffness of buildings, to identify the damaged point of buildings for each frame.

INTRODUCTION

The largest damage to buildings may be due to earthquakes in the lifespan. Recently, reducing the environmental impacts has become the significant social demand. We are compelled to live in the buildings for a long time by repairing or reforming. To use them, we need a reliable method that identifies the damaged point of buildings. The damaged point is suggested by fluctuations of stiffness and attenuation. A stiffness and attenuation of buildings are called "dynamic characters of buildings".

After the Kobe earthquake of 1995 occurred, estimating the dynamic character of buildings from micro-tremors has been studied. But, almost all of these studies only focus on the transformation of natural period of buildings, while the studies for each of the frame of buildings are limited. Many buildings are low storied in Japan, so we need a dynamic character of each frame of the buildings because they are eccentric ones.

Dynamic character of buildings consists of stiffness and attenuation obtained by modeling buildings to multi-mass system model. We identify the stiffness and attenuation of each frame of the building by using Generic Algorithm in order to fit transfer functions of theoretical equation of motions to transfer functions of observed micro-tremors. The advantage of observing micro-tremors is that we can non-destructively estimate the dynamic characters and observe micro-tremors at any buildings at any time. If we identify the reliable stiffness and attenuation of each frame of the building, we can use an effective method for our purpose described ahead.

However, when we identify the reliable stiffness and attenuation, and perform reverse Fourier transforms directly to transfer functions retrieved from micro-tremors, we encounter the situation where the Green's function does not satisfy causality. As things are, the identified stiffness and attenuation is not reliable. Then, we retrieve Green's functions from transfer functions of micro-tremors that satisfy the causality by transforming phase spectra. We are able to survey the reliable stiffness of each frame of buildings by using this Green's function. We check whether the estimated Green's function is valid or not by visualizing the linear response at an arbitrary floor using a frame model of the building.

Our objective is to suggest the method to identify the damage point of buildings. This study is divided into three steps. The first step is to estimate the transfer function of the building by observing the micro-tremor. The second step is to retrieve the Green's function that satisfies causality. The final step is to identify the stiffness and attenuation of each frame of the building. The final step only target for the stiffness of the building. The attenuation of the building is given by the stiffness as the proportional attenuation. We study the possibility of this method through these steps. The target of our study is building #10 of the Osaka Institute of Technology with large eccentricity in terms of the gravity centre.

TRANSFER FUNCTION ESTIMATED FROM MICROTREMORS

The Method of Observation

We observed micro-tremors at building #10 of the Osaka Institute of Technology with large eccentricity in terms of the gravity centre. The building #10 is eccentric structure made by steal except the part of underground structure which is made by SRC, and the building itself is genuine rigid frame. The building #10 has 12 floors above the ground and a basement floor. To avoid noises caused by activity of people and traffic, we performed the observation of micro-tremors from midnight till early morning. We observed for 30 minutes and sampling time was 0.01 second, and analog high-cut filter was 5 Hz.

Figure 1 shows the observation point on the plan of ground floor, and Fig. 2 shows the observation point on the plan of other floors. The circle mark is the gravity centre, and the triangle mark is rigid centre, and the box mark is observation point shown in Fig. 1 and Fig. 2. We set four observation instruments on the ground floor including the gravity centre and three observation instruments on the other floors.

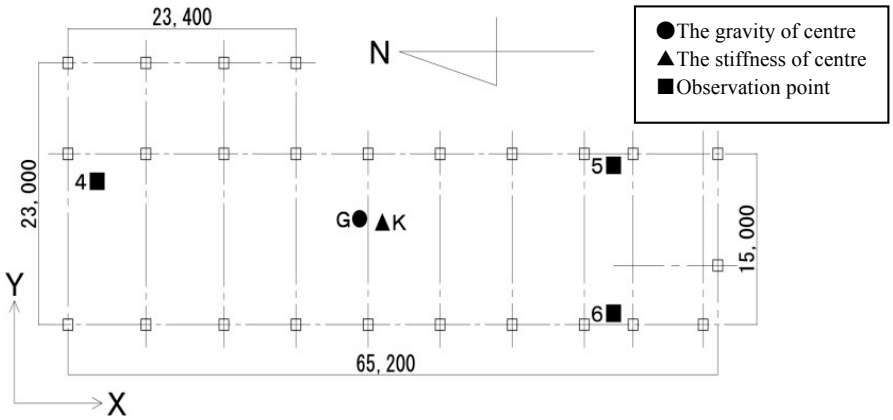

(a) Ground floor

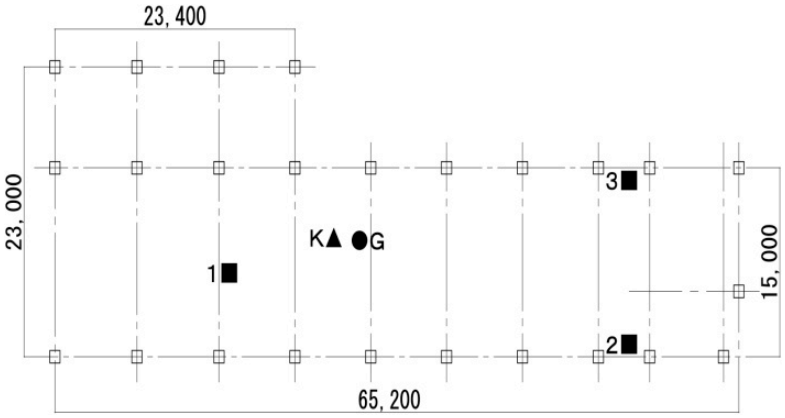

(b) Other floor except basement floor

Fig. 1. Observation points on the plan of building #10 of (a) ground floor and (b) other floor except basement floor.

Transfer Functions Estimated from the Micro-tremor of the Building #10

Movement of translation of optional point **r** on the X-Y plane (floor plane) is expressed as,

$$V_X^r(t) = V_X(t) - \omega_Z(t) y_r \tag{1}$$

$$V_Y^r(t) = V_Y(t) + \omega_Z(t) x_r, \tag{2}$$

when the floor is rigid. Here, $V_x(t)$ and $V_Y(t)$ is velocity of translation of X and Y direction on the gravity centre, respectively, and $\omega_z(t)$ is velocity of rotational angle. Incidentally, these functions define the time domain. We are able to estimate two component of translation and a component of rotational angle, calculating simultaneous equations lead from conditions which minimize square residuals of velocity $V_x^r(t)$, $V_Y^r(t)$ (Eqs. 1 and 2) and velocity of X and Y direction $O_x^r(t)$, $O_Y^r(t)$ obtained from observed micro-tremors. These conditions which minimize square residuals are showed in Eqs. 3, 4, and 5. These equations are partial differential equations for $V_x(t)$, $V_Y(t)$, and $\omega_z(t)$.

$$\frac{\partial f}{\partial V_X(t)} = -2\sum_{j=1}^{m}\left\{O_X^{rj}(t) - V_X(t) + \omega_Z(t) y_{rj}\right\} = 0 \tag{3}$$

$$\frac{\partial f}{\partial V_Y(t)} = -2\sum_{j=1}^{m}\left\{O_Y^{rj}(t) - V_Y(t) - \omega_Z(t) x_{rj}\right\} = 0 \tag{4}$$

$$\begin{aligned}\frac{\partial f}{\partial \omega_Z(t)} &= 2\sum_{j=1}^{m}\left\{O_X^{rj}(t) - V_X(t) + \omega_Z(t) y_{rj}\right\} y_{rj} \\ &\quad -2\sum_{j=1}^{m}\left\{O_Y^{rj}(t) - V_Y(t) - \omega_Z(t) x_{rj}\right\} x_{rj} = 0\end{aligned} \tag{5}$$

We get the two component of translation and a component of rotational angle, to calculate the simultaneous equation which is made of Eqs. 3, 4, and 5. Figure 2 shows the velocity waveform of the two component of translation and a component of rotational angle of the building #10.

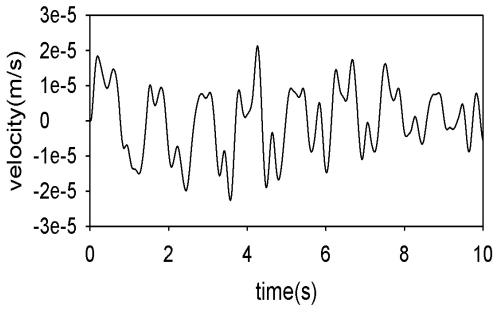

(a) *The velocity waveform of translation of X direction.*

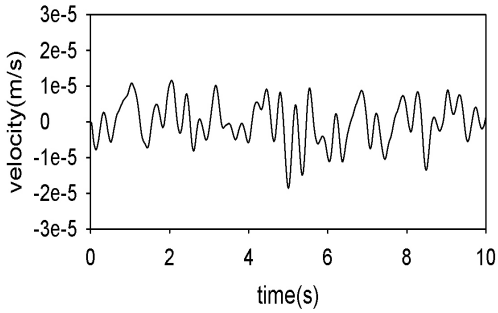

(b) *The velocity waveform of translation of Y direction.*

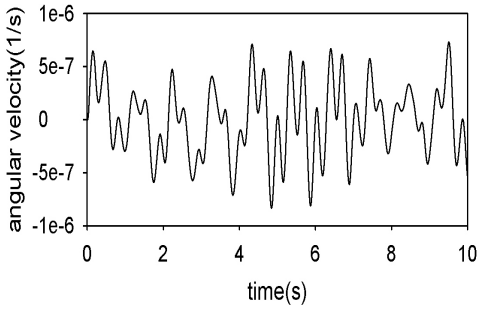

(c) *The velocity waveform of rotational angle rotate Z axis.*

Fig. 2. The velocity waveform of translation and rotational angle isolated from the micro-tremors.

Figure 2a is the velocity waveform of translation of X direction, and Fig. 2b is the velocity waveform of translation of Y direction. Also Fig. 2c is the velocity waveform of rotational angle rotate Z axis. If it is a transient wave like a seismogram, we can perform Fourier transforms directly to $V_X(t)$, $V_Y(t)$, and $\omega_Z(t)$. However, these are not a transient wave but a standing wave. So we cannot perform Fourier transforms directly. We need to develop the simultaneous equation by performing Fourier transforms. The correlation function is estimated from auto-correlation and cross-correlation; the auto-correlation is calculated by the mutual ground motion at the gravity centre, and the cross-correlation is done by the mutual floor motion and ground motion there. The simultaneous equation that calculates the response for X-direction input is expressed by Eq. 6 in the frequency domain. In Eq. 6, the matrix on the left side has 9 components of cross-correlation. The row vector on the left side that has 3components of the transfer function is our target, and the row vector on the right side has 3 components of auto-correlation. In the same way, the simultaneous equation that calculates the response for Y-direction input is expressed by Eq. 7, and the simultaneous equation that calculates the response for Z-axis rotation is expressed by Eq. 8 in the frequency domain. "~" shows conjugate complex number.

$$\begin{bmatrix} S_{\dot{x}_0\dot{x}_0}(\omega) & S_{\dot{x}_0\dot{y}_0}(\omega) & S_{\dot{x}_0\dot{\theta}_0}(\omega) \\ S_{\dot{y}_0\dot{x}_0}(\omega) & S_{\dot{y}_0\dot{y}_0}(\omega) & S_{\dot{y}_0\dot{\theta}_0}(\omega) \\ S_{\dot{\theta}_0\dot{x}_0}(\omega) & S_{\dot{\theta}_0\dot{y}_0}(\omega) & S_{\dot{\theta}_0\dot{\theta}_0}(\omega) \end{bmatrix} \times \begin{Bmatrix} \tilde{H}_{xx}(\omega) \\ \tilde{H}_{xy}(\omega) \\ \tilde{H}_{x\theta}(\omega) \end{Bmatrix} = \begin{Bmatrix} S_{\dot{x}_i\dot{x}_0}(\omega) \\ S_{\dot{x}_i\dot{y}_0}(\omega) \\ S_{\dot{x}_i\dot{\theta}_0}(\omega) \end{Bmatrix} \tag{6}$$

$$\begin{bmatrix} S_{\dot{x}_0\dot{x}_0}(\omega) & S_{\dot{x}_0\dot{y}_0}(\omega) & S_{\dot{x}_0\dot{\theta}_0}(\omega) \\ S_{\dot{y}_0\dot{x}_0}(\omega) & S_{\dot{y}_0\dot{y}_0}(\omega) & S_{\dot{y}_0\dot{\theta}_0}(\omega) \\ S_{\dot{\theta}_0\dot{x}_0}(\omega) & S_{\dot{\theta}_0\dot{y}_0}(\omega) & S_{\dot{\theta}_0\dot{\theta}_0}(\omega) \end{bmatrix} \times \begin{Bmatrix} \tilde{H}_{yx}(\omega) \\ \tilde{H}_{yy}(\omega) \\ \tilde{H}_{y\theta}(\omega) \end{Bmatrix} = \begin{Bmatrix} S_{\dot{y}_i\dot{x}_0}(\omega) \\ S_{\dot{y}_i\dot{y}_0}(\omega) \\ S_{\dot{y}_i\dot{\theta}_0}(\omega) \end{Bmatrix} \tag{7}$$

$$\begin{bmatrix} S_{\dot{x}_0\dot{x}_0}(\omega) & S_{\dot{x}_0\dot{y}_0}(\omega) & S_{\dot{x}_0\dot{\theta}_0}(\omega) \\ S_{\dot{y}_0\dot{x}_0}(\omega) & S_{\dot{y}_0\dot{y}_0}(\omega) & S_{\dot{y}_0\dot{\theta}_0}(\omega) \\ S_{\dot{\theta}_0\dot{x}_0}(\omega) & S_{\dot{\theta}_0\dot{y}_0}(\omega) & S_{\dot{\theta}_0\dot{\theta}_0}(\omega) \end{bmatrix} \times \begin{Bmatrix} \tilde{H}_{\theta x}(\omega) \\ \tilde{H}_{\theta y}(\omega) \\ \tilde{H}_{\theta\theta}(\omega) \end{Bmatrix} = \begin{Bmatrix} S_{\dot{\theta}_i\dot{x}_0}(\omega) \\ S_{\dot{\theta}_i\dot{y}_0}(\omega) \\ S_{\dot{\theta}_i\dot{\theta}_0}(\omega) \end{Bmatrix} \tag{8}$$

In Eqs. 6, 7, and 8, the symbol $S_{\dot{j}_0\dot{k}_0}$ expresses power spectrum of j-direction output for k-direction input at the ground floor, and the symbol $S_{\dot{j}_i\dot{k}_0}$ expresses power spectrum of j-direction output of optional i-floors ($i = 1,2,3,\cdots,N$) for k-direction input at the ground floor. H_{jk} is the transfer function of j-direction output of optional i-floors ($i = 1,2,3,\cdots,N$) for k-direction input. We obtained the transfer function by computing the simultaneous equations of the Eqs. 6, 7, and 8, and note that each of the matrix of Eqs. 6, 7, and 8 are the same. Figure 3 shows the transfer functions H_{jk} of the 11th floor. The horizontal line shows frequency, and the vertical line shows transfer function.

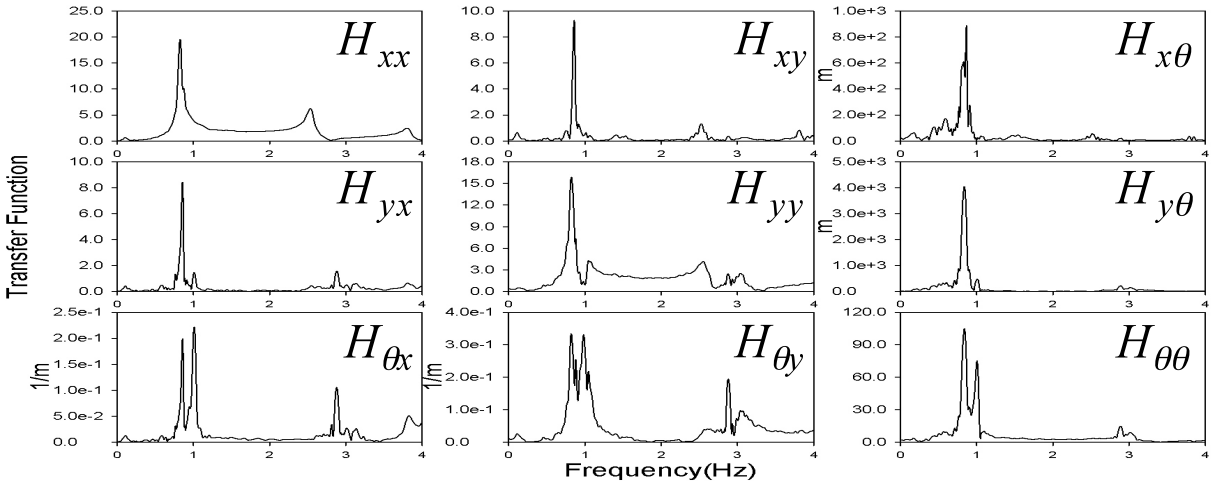

Fig. 3. Transfer function retrieved from the micro-tremor.

Each of the transfer function of Eqs. 6, 7, and 8 is expressed in Eq. 9. Transfer function is showed by the participation vector and the eigenvalue, as the floor is rigid, and the linear response.

$$\left\{H_{jk}^{i}(\omega)\right\}=(i\omega^2)\sum_{s=1}^{3N}\left[s\beta k\cdot\left\{{}_{s}U_{j}^{i}\right\}\right]\frac{1}{i\omega-s\lambda}+(i\omega^2)\sum_{s=1}^{3N}\left[s\tilde{\beta}k\cdot\left\{{}_{s}\tilde{U}_{j}^{i}\right\}\right]\frac{1}{i\omega-s\tilde{\lambda}} \tag{9}$$

Here, the symbol s is mode degree ($s=1,2,3,\cdots,3N$) as N is number of all floors, the symbol j is output direction ($j=1,2,3$ corresponds X,Y,θ), the symbol k is input direction ($k=1,2,3$ corresponds X,Y,θ), the affixing character ι is floor number ($\iota=1,2,3,\cdots,N$), the symbol i is unit imaginary number, $s\beta k\cdot\left\{{}_{s}U_{j}^{i}\right\}$ is the participation vector, and $s\lambda$ is the eigenvalue.

RETRIVING THE GREEN'S FUNCTION

The Causality

The linear response of earthquake motions is showed below in Eq. 10 in the time domain. This Eq. 10 expresses the torsional vibration (Koh, *et al*., 1969). We calculate the vibration equation using the Foss's method (Foss, 1958). The symbol "*" shows convolutions in the left side. In Eq. 10, the matrix on the left side is 9 components of Green's functions of an optional floor, the row vector on the left side is 3components of earthquake motions inputted the ground floor of the building, and the row vector on the right side is 3 components of response of earthquake motions of an optional floor.

$$\begin{bmatrix}\left\{g_{xx}^{i}(t)\right\} & \left\{g_{xy}^{i}(t)\right\} & \left\{g_{x\theta}^{i}(t)\right\}\\ \left\{g_{yx}^{i}(t)\right\} & \left\{g_{yy}^{i}(t)\right\} & \left\{g_{y\theta}^{i}(t)\right\}\\ \left\{g_{\theta x}^{i}(t)\right\} & \left\{g_{\theta y}^{i}(t)\right\} & \left\{g_{\theta\theta}^{i}(t)\right\}\end{bmatrix}*\begin{Bmatrix}\ddot{x}_0(\tau)\\ \ddot{y}_0(\tau)\\ \ddot{\theta}_0(\tau)\end{Bmatrix}=\begin{Bmatrix}\left\{x^{i}(t)\right\}\\ \left\{y^{i}(t)\right\}\\ \left\{\theta^{i}(t)\right\}\end{Bmatrix} \tag{10}$$

Each of the Green's function of the Eq. 10 is showed by Eq. 11. This Green's function is obtained by performing reverse Fourier transforms to Eq. 9. The second term is conjugate complex number of the first term. This Green's function is consists of a participation vector and an eigenvalue. Each of the symbol and coefficient is the same as Eq. 9.

$$\left\{g_{jk}^{i}(t)\right\}=\frac{(i\omega)^2}{2\pi}\cdot\sum_{s=1}^{3N}\left[s\beta\cdot\left\{{}_{s}U_{j}^{i}\right\}\right]\int_{-\infty}^{\infty}\frac{1}{i\omega-s\lambda}\cdot e^{i\omega t}d\omega+\frac{(i\omega)^2}{2\pi}\cdot\sum_{s=1}^{3N}\left[s\tilde{\beta}\cdot\left\{{}_{s}\tilde{U}_{j}^{i}\right\}\right]\int_{-\infty}^{\infty}\frac{1}{i\omega-s\tilde{\lambda}}\cdot e^{i\omega t}d\omega \tag{11}$$

In Eq. 11, a singularity is obtained from the eigenvalue at the part of complex integration ($\omega=-i\cdot s\lambda$). On the complex plane, the causality of Green's functions is filled if the singularity is on the upper half-plane. We can satisfy the causality by imposing the condition on the real part of eigenvalue which is less than 0 ($\mathrm{Re}[s\lambda]<0$). We can read the peak point of transfer functions from transfer functions estimated from micro-teremors (see Fig. 4). Because a peak point is the same as each mode s of $|s\lambda|$, we are able to reduce the variable by fixing these peak point.

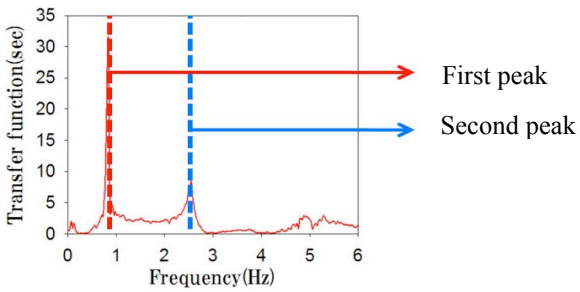

Fig. 4. Sample of transfer function estimated from micro-tremors.

The method that we identify the participation vector and eigenvalue by fitting transfer functions of theoretical equation of motions to transfer functions of observed micro-tremors is able to easily introduce the condition described ahead. And this method is direct method. Used mode is to the third mode because we can confirm a peak to the third mode from the micro-tremor. Number of generations is 21000, number of chromosome is 120, number of crossing rate is 0.25, and number of mutate rate is 0.01. Standard value of identified variable is obtained from the transfer function estimated from the optimal stiffness etc., and range of retrieval is almost from 0.9 times to 1.1 times.

Figure 5 compares the Green's function estimated from the micro-tremor to the Green's function estimated from the identified transfer function. The figure on the left side is former, and the figure on the right side is latter. The horizontal axis shows the time, and the vertical axis shows the Green's function. If you compare both, you can see the improvement of the causality clearly.

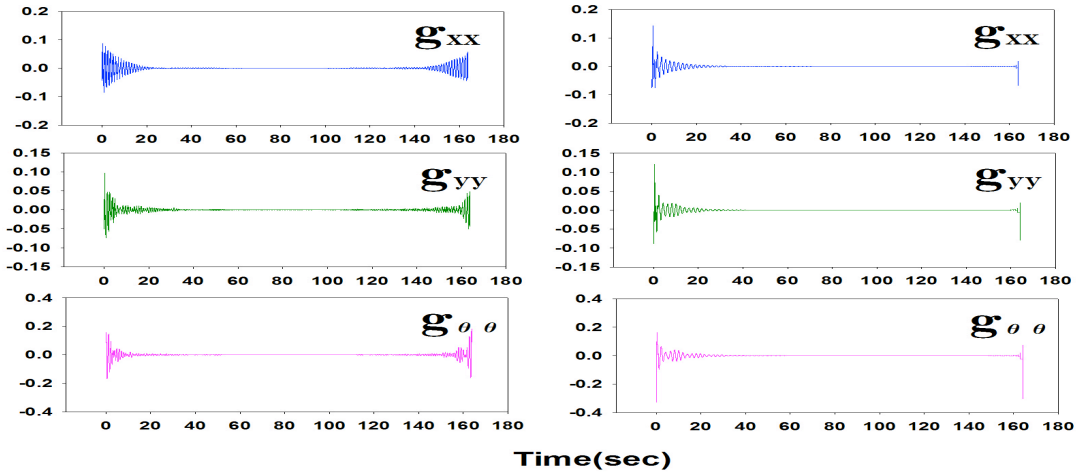

(a) estimated from micro-tremor (b) estimated from identified transfer function

Fig.5. Check the causality of Green's function (a) estimated from micro-tremor and (b) estimated from identified transfer function.

Retrieving the Green's Function

Figure 6 shows the fitting result of the 12th floor according to the expression of Eq. 10. In Fig. 6, solid line shows the transfer function estimated from the micro-tremor, broken red line shows the identified transfer function. Position and value of amplitude of first mode match well, and those of second mode match to some extent.

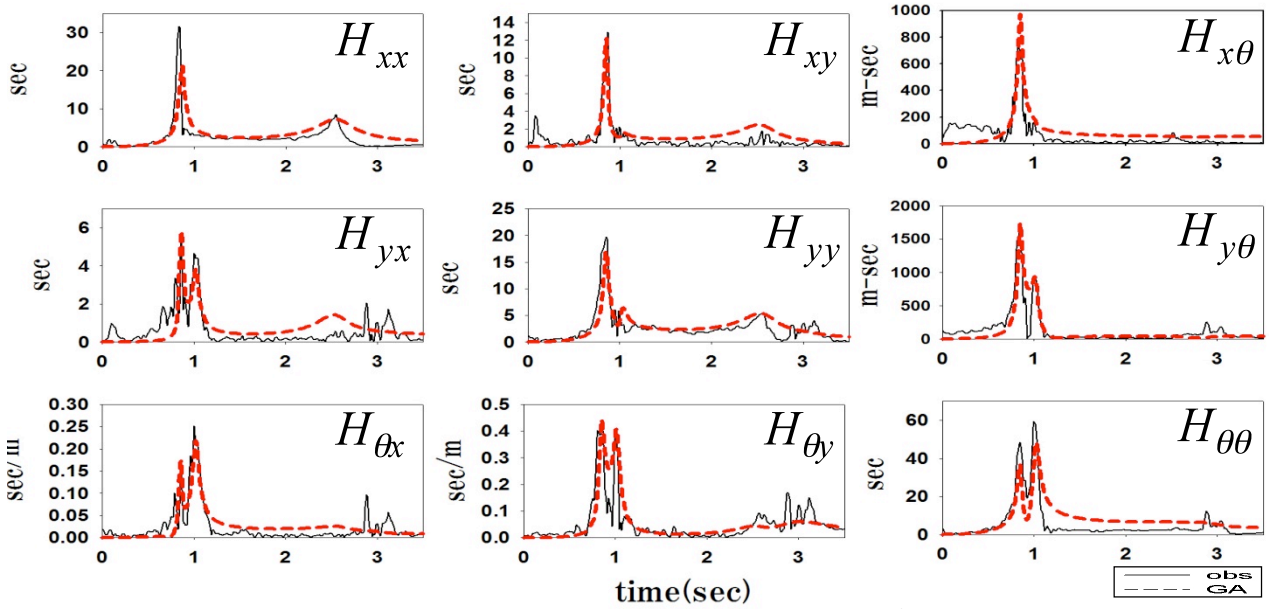

Fig.6. The fitting result of two Green's function for 12th floor.

Figure 7 compares the estimated Green's function and the Green's function calculated by Eq. 11 using the structural design data. It is according to expression of Eq. 10. The broken line shows former, and the solid line shows latter. On the g_{xy} and g_{yx}, it suggests the coupling effect because the broken line is greater than the straight line. The coupling effect signifies the interaction which vibration of X (Y) direction is occurred by Y (X) direction input. This coupling effect is seen at the each floor. On the $g_{x\theta}$ and $g_{y\theta}$, the broken line shows about 10 times the value of the straight line. So we think response of earthquake by the influence of rotation input is large.

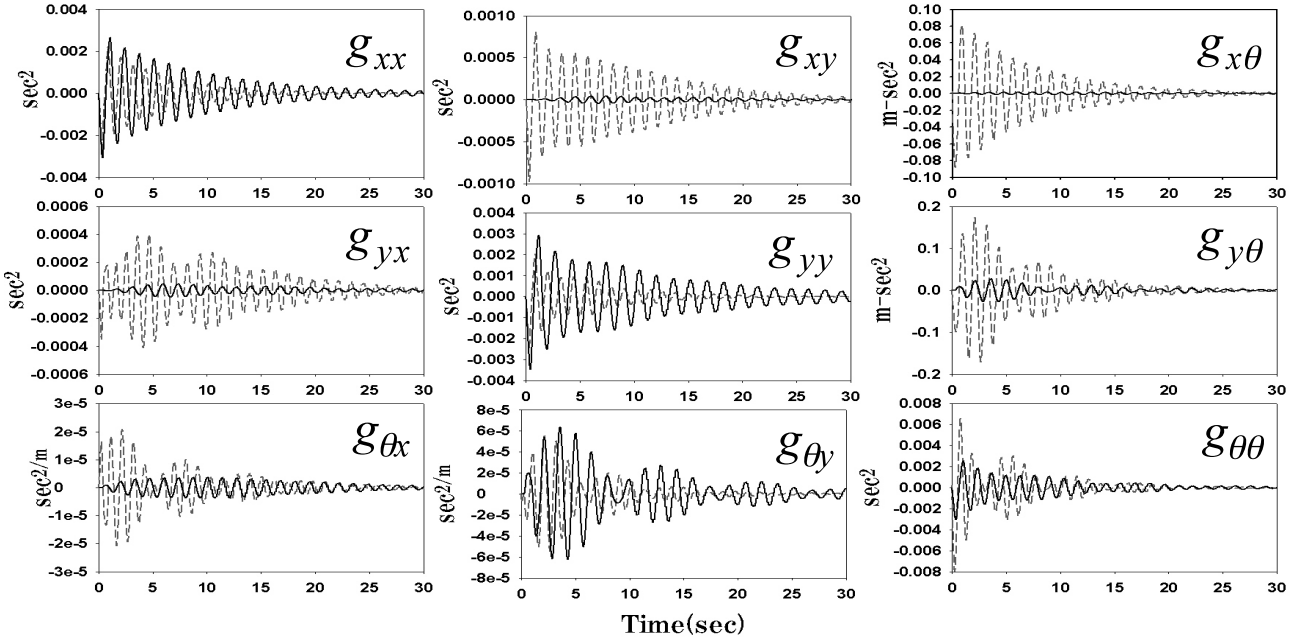

Fig.7. Compare the Green's function for 12th floor.

Visualizing the linear response

Figure 8 shows the linear response of the building #10 that was calculated by estimated Green's functions and input earthquakes. The building #10 is showed by using a frame model of the building. The upper figures are input earthquakes of X-direction, Y-direction, and rotation. The bottom left figure shows the linear response of the building #10, the bottom right figure is top of the view. By looking at Fig. 8, we can understand that the building #10 vibrates rotationally. And, we think that each transformation is appropriate.

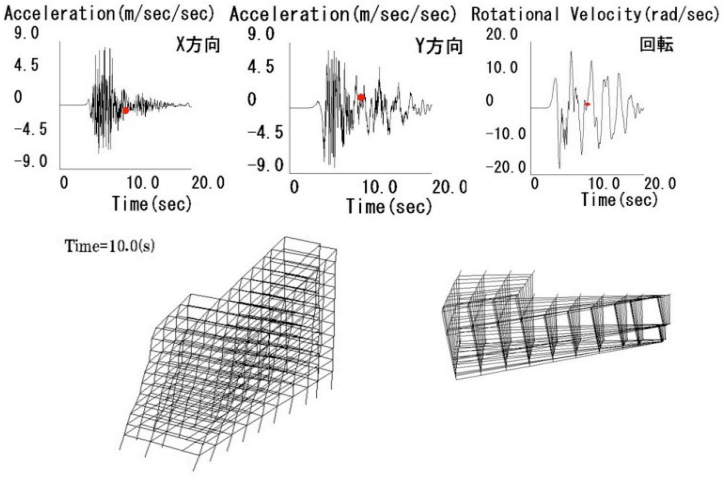

Fig.8. Linear response of building #10 (t=10.0(sec)).

IDENTIFYING THE STIFFNESS OF THE BUILDING

The Method of Identification

In the preceding chapter, we checked that we are able to estimate the appropriate Green's function that satisfied causality. Thus, in this chapter, using Generic Algorithm (Holland, 1975), we try to identify the parameter of dynamic character by fitting transfer functions calculated by vibration equation (the calculated transfer function) and transfer functions estimated from micro-tremors (the observed transfer functions). The parameters of dynamic character are 6 parameters that are the mass (M) and moment of inertia (I) of the each floor and the stiffness (${}_iK_x \cdot {}_iK_y$) and attenuation (${}_iC_x \cdot {}_iC_y$) of the each frame.

The fitness function generally is used to measure the fitness as reverse value of residuals of two functions that is the calculated transfer function and the observed transfer functions. If you use this method, there is danger of identifying an improper parameter because we identify the 9 components of transfer function that has different unit. To solve this problem, we use Eq. 12.

$$f = \sum_{\omega=1}^{N} \frac{1}{\left| \frac{obs(\omega) - cal(\omega)}{obs_{\max}} \right| + 1} \tag{12}$$

In Eq. 12, N is sample value of transfer functions, f is fitness, and obs is the observed transfer functions. Cal is the calculated transfer function, $obs_{\max}$ is max value of observed transfer functions and Eq. 12 is divided residuals of two functions. They are the calculated transfer function and the observed transfer functions by each max value of the observed transfer functions. The natural frequency regions up to the second are in the range of the evaluation.

We need to determine the standard value and identify the parameters of dynamic character. We take the mass M from the earthquake load that is used on the structure design of the building #10. The moment of inertia is calculated from the mass M and the shape of floor. The stiffness K is calculated from stress analyses. We use the stiffness K to calculate the attenuation C. Search range is determined by preliminary identify result. Table 1 shows the search range. In GA, we set the number of generation, which is 30000 and the number of chromosome is 100, the bit is 6 bit, the cross probability is 0.25, and the mutation probability is 0.05.

Table 1. Search range for parameters of dynamic character.

1~11 floor	Min	Standard Value	Max
M(kg)	1.0	M	1.2
I(kg·m^2)	0.9	I	1.1
${}_iK_x$(N/m)	1.1	${}_iK_x$	1.5
${}_iK_y$(N/m)	1.3	${}_iK_y$	1.7
${}_iC_x$(Ns/m)	8.33E-03	${}_iK_x$	5.00E-02
${}_iC_y$(Ns/m)	6.25E-03	${}_iK_y$	3.33E-02

The Result of Identification

Figure 9 is comparing the observed transfer functions and the transfer function that is calculated by the identified dynamic characters. The amplitude of transfer function is approximately the same. We think we are able to identify reliable for the stiffness that effects the position of natural frequency, because the position of first natural frequency is the same. But, it is difficult to identify the components of rotation and the second natural frequency and higher. It is caused by the transit wave input, e.g. wind. We need to think about this problem because wind is also the cause about the causality. We could not use Eq. 10 of the state equation in time domain. This identification is calculated by using the CFT to reduce the calculating time. The CFT is one of the Discrete Fourier Transforms. We use the subroutine program is called the CFT at SSL‡Ų. (If you don't use the CFT, it will take you 140 times as much time as you think). That is why Fig. 9 is different from Fig. 6.

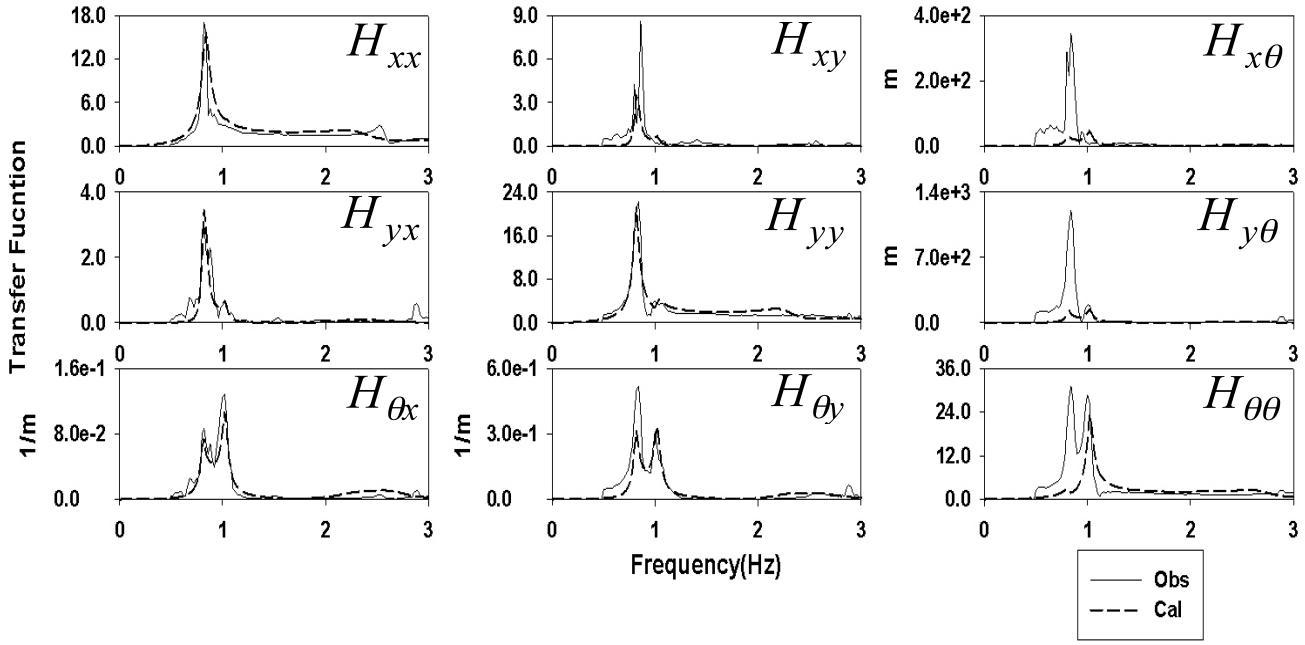

Fig. 9. Fitting result of the transfer function.

Especially, in Fig. 9, $H_{x\theta}$ and $H_{y\theta}$ is not much. This might be caused by the wind. Identified stiffness K is expressed by constant times of standard value (see Table 2 or Table 3). In Tables 2 and 3, the stiffness is increased for any stiffness. We think that one of these reasons is to influence the non-structure materials such as a partitioning wall.

Table 2. The identified stiffness ${}_iK_y$ (Short direction).

Short Direction Stiffness ${}_iK_y$											
Floor	**X1 frame**	**X2 frame**	**X3 frame**	**X4 frame**	**X5 frame**	**X6 frame**	**X7frame**	**X8 frame**	**X9 frame**	**X10 frame**	**X11 frame**
1	1.65	1.70	1.70	1.70	1.70	1.70	1.67	1.35	1.30	1.30	1.30
2	1.62	1.57	1.35	1.52	1.55	1.66	1.57	1.40	1.55	1.31	1.30
3	1.70	1.63	1.49	1.70	1.69	1.38	1.65	1.59	1.67	1.35	1.50
4	1.69	1.62	1.65	1.67	1.69	1.61	1.59	1.60	1.43	1.38	1.59
5	1.67	1.67	1.70	1.67	1.62	1.68	1.65	1.45	1.48	1.36	1.64
6	1.70	1.68	1.39	1.47	1.60	1.34	1.63	1.54	1.50	1.50	1.70
7	1.50	1.44	1.55	1.30	1.33	1.55	1.58	1.60	1.48	1.60	1.40
8	1.61	1.36	1.30	1.33	1.30	1.30	1.31	1.43	1.33	1.34	1.38
9	1.30	1.30	1.35	1.30	1.30	1.30	1.30	1.52	1.34	1.46	1.31
10	1.50	1.31	1.30	1.31	1.31	1.33	1.30	1.40	1.33	1.41	1.34
11	1.34	1.31	1.30	1.30	1.36	1.30	1.34	1.33	1.30	1.32	1.30

Table 3. The identified stiffness ${}_iK_y$ (Long direction).

Long direction Stiffness ${}_iK_x$				
Floor	**Y1 frame**	**Y2 frame**	**Y3 frame**	**Y4 frame**
1	1.50	1.50	1.32	1.24
2	1.50	1.50	0.00	1.22
3	1.49	1.47	1.25	1.12
4	1.49	1.49	1.50	1.12
5	1.42	1.50	1.33	1.11
6	1.49	1.46	1.40	1.16
7	1.50	1.40	1.15	1.10
8	1.37	1.21	1.10	1.10
9	1.50	1.24	1.17	1.10
10	1.50	1.28	1.30	1.10
11	1.47	1.49	1.32	1.10

CONCLUSION

The following conclusions may be stated from the results.

(1) It is possible to retrieve the Green's function that satisfies causality.
(2) The Green's function has a coupling effect.
(3) It is possible to identify the parameters of dynamic character of each floor and each frame.
(4) We are able to confirm the condition of the building by using these methods.

ACKOWLEGEMENT

This study received great assistance from Y. Takayasu for identifying the parameter of dynamic character, and we had a deeper discussion by his sagacious view. Also, this study received great assistance from S. Takemura for calculating the transfer function from observed micro-tremors. And, this study received great assistance from T. Hashime for checking effectiveness of the program code. We are deeply grateful to Y. Takayasu, S. Takemura, and T. Hashime.

REFERENCES

Foss, K. A. [1958]. "Co-ordinates which uncouple the equations of motion of damped linear dynamic systems", ASME Journal of Applied Mechanics, 25, pp.361-364.

Koh, T., H. Takase, and T. Tsugawa [1969]. "Torsional Problems in Aseismic Design of High-rise Buildings", IV WCEE, Santiago, A4-71.

Holland, J. H. [1975]. "*Adaptation in Natural and Artificial Systems*", University of Michigan Press.